

# PROCEEDINGS OF SPIE

[SPIDigitalLibrary.org/conference-proceedings-of-spie](https://spiedigitallibrary.org/conference-proceedings-of-spie)

## Photoluminescence properties of ZnSe:Al, ZnSe:Cu nanoparticles obtained by chemical synthesis

Irina V. Tepliakova, Yury A. Nitsuk, Ievgen V. Brytavskiy, Andrzej Kociubiński, Meruyert Sakypbekova

Irina V. Tepliakova, Yury A. Nitsuk, Ievgen V. Brytavskiy, Andrzej Kociubiński, Meruyert Sakypbekova, "Photoluminescence properties of ZnSe:Al, ZnSe:Cu nanoparticles obtained by chemical synthesis," Proc. SPIE 11176, Photonics Applications in Astronomy, Communications, Industry, and High-Energy Physics Experiments 2019, 111764M (6 November 2019); doi: 10.1117/12.2536248

**SPIE.**

Event: Photonics Applications in Astronomy, Communications, Industry, and High-Energy Physics Experiments 2019, 2019, Wilga, Poland

# Photoluminescence Properties of ZnSe:Al, ZnSe:Cu Nanoparticles Obtained by Chemical Synthesis

Irina V. Tepliakova<sup>a</sup>, Yury A. Nitsuk<sup>a</sup>, Ievgen V. Brytavskiy<sup>a</sup>, Andrzej Kociubiński\*<sup>b</sup>, Meruyert Sakypbekova<sup>c</sup>

<sup>a</sup>I.I.Mechnikov Odessa National University, Dvoryanskaya Str., 2, 65082 Odessa, Ukraine; <sup>b</sup>Lublin University of Technology, Nadbystrzycka 38D, 20-618 Lublin, Poland; <sup>c</sup>Al-Farabi Kazakh National University, Al-Farabi 71 Avenue, Almaty, Republic of Kazakhstan

## ABSTRACT

This work represents an effective method for synthesis and doping of ZnSe nanocrystals with elements of group 3 and transition elements. The structure of crystals and their average size are determined. The spectra of optical density and photoluminescence were studied, and a comparative analysis of characteristics of the obtained nanoparticles with their bulk analogs was carried out.

**Keywords:** ZnSe nanoparticles, photoluminescence, optical properties, biomedical labeling, luminescent labels, colloidal synthesis

## 1. INTRODUCTION

Semiconductor nanocrystals of A2B6 group are promising materials for semiconductor electronics, biomedical imaging and disinfection. Existing synthesis methods make it possible to obtain nanocrystals with a narrow size distribution, specified surface morphology and high stability. The ability to control the band gap and the luminescence wavelength makes these nanocrystals useful for optoelectronics. Luminescent semiconductor nanoparticles with wide absorption spectrum and pronounced luminescence peaks in the visible and near-IR regions are very promising for medical diagnostics [1].

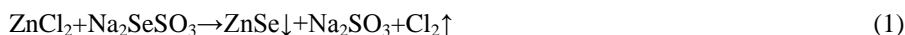
Among the semiconductor crystals of the A2B6 group, the most studied are CdS and CdSe. Cheap and simple method of obtaining, as well as high quantum yield of radiation in the visible region of the spectrum can be mentioned as the main advantages of these materials [1,2,3]. A serious disadvantage of these materials is their cytotoxicity. Therefore, it is advisable to use nanocrystals of selenide and zinc sulfide for biomedical applications. In order to be used as markers for fluorescence tomography, nanocrystals must have effective radiation in red and near-IR regions [4,5,6]. It is known that aluminum and copper impurities are effective activators of radiation in these regions in bulk ZnSe crystals. Therefore, the study of the optical and luminescent properties of ZnSe:Al and ZnSe:Cu nanocrystals is relevant [7,8].

## 2. FORMULATION OF THE PROBLEM

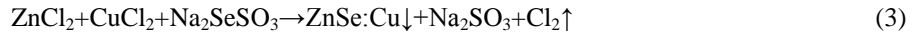
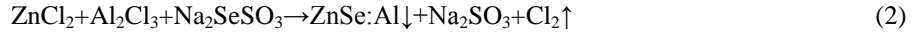
The purpose of this work is to find a way to control the spectral position of the longwave radiation bands of ZnSe nanocrystals by doping them with aluminum and copper impurities, to establish the nature of optical and luminescent transitions in ZnSe, ZnSe:Al and ZnSe:Cu nanocrystals.

## 3. MAIN RESEARCH MATERIAL

In this work, zinc selenide nanocrystals were studied, which were obtained by a chemical method using commercial reagents from the Merck Company. The source of zinc ions was zinc chloride, and the source of selenium ions was sodium selenosulfate. For doping with aluminum or copper, a 1% solution of aluminum chloride or copper chloride was added to a 10% solution of zinc chloride. The synthesis of nanoparticles was carried out in 1 ml of a 5% gelatin solution and had the following form [8,9,10]:



\*akociub@semiconductor.pl



After removing residual reaction products, a colloidal solution of nanoparticles was deposited on a quartz substrate and placed in an oven until the polymer film dried. For X-ray diffraction and SEM studies, the solution was deposited on silicon substrates. On X-ray diffractograms, the dominant peaks were identified, which correspond to the (111), (220), (311) planes in ZnSe (Fig. 1, according to JCPDS 96-900-8858). Similar planes were found in ZnSe: Al and ZnSe: Cu nanocrystals.

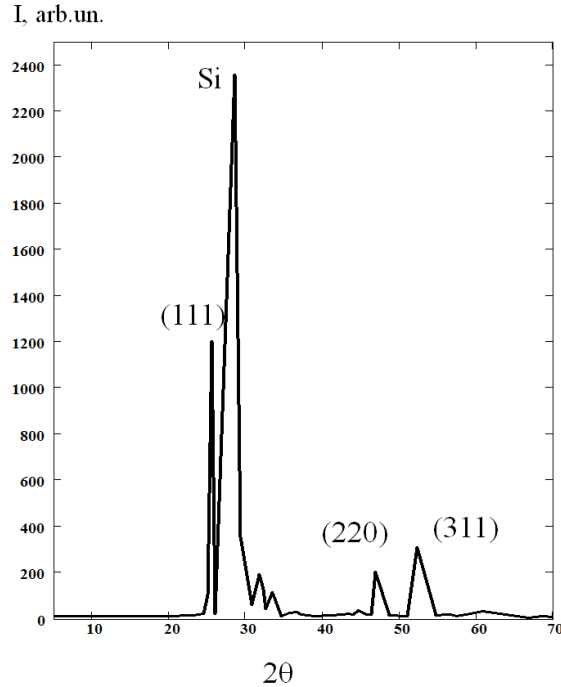


Figure 1. XRD image of ZnSe nanocrystals

Tabela 1. Optical characteristics of ZnSe, ZnSe:Al, ZnSe:Cu nanocrystals in region of optical absorption edge

Sample	The type of nanocrystals	$E_g$ , eV	$\Delta E_g$ , eV	$R$ , nm
1	ZnSe, 0.05% ZnCl <sub>2</sub> , 0.05% Na <sub>2</sub> SeSO <sub>3</sub>	3.63	0.95	4.3
2	ZnSe, 0.03% ZnCl <sub>2</sub> , 0.03% Na <sub>2</sub> SeSO <sub>3</sub>	3.78	1.1	4
3	ZnSe:Al, 0.03% ZnCl <sub>2</sub> +0.001% Al <sub>2</sub> Cl <sub>3</sub> , 0.03% Na <sub>2</sub> SeSO <sub>3</sub>	3.76	1.08	4.1
4	ZnSe:Al, 0.03% ZnCl <sub>2</sub> +0.002% Al <sub>2</sub> Cl <sub>3</sub> , 0.03% Na <sub>2</sub> SeSO <sub>3</sub>	3.71	1.03	4.2
5	ZnSe:Cu, 0.05% ZnCl <sub>2</sub> +0.001% CuCl <sub>2</sub> , 0.05% Na <sub>2</sub> SeSO <sub>3</sub>	3.54	0.86	4.6
6	ZnSe:Cu, 0.05% ZnCl <sub>2</sub> +0.002% CuCl <sub>2</sub> , 0.05% Na <sub>2</sub> SeSO <sub>3</sub>	3.44	0.76	4.8
7	ZnSe:Cu, 0.05% ZnCl <sub>2</sub> +0.003% CuCl <sub>2</sub> Cl <sub>3</sub> , 0.05% Na <sub>2</sub> SeSO <sub>3</sub>	3.38	0.7	5

For comparison, bulk ZnSe, ZnSe: Al and ZnSe: Cu crystals obtained by diffusion doping of Al and Cu impurities at various temperatures of growth were studied. The temperature varied from 750 to 900°C.

The optical density and photoluminescence spectra were investigated to establish the nature of optical and luminescent transitions in studied nanocrystals as well as to determine the average size of nanoparticles and the concentration of an optically active impurity. For this purpose, the sets of samples with different ratio of initial and impurity components were selected (Table 1).

The optical density spectra were measured using a MDR-6 monochromator with diffraction gratings of 2400 lines/mm for the ultraviolet, 1200 lines/mm for the visible and near-IR spectral regions and 600 lines/mm for the IR region. A photomultiplier tube FEU-100 was used as a radiation detector. The photoluminescence spectra were measured on an ISP-51 prism spectrograph. The registration of radiation was carried out with a FEU-100 photomultiplier tube and IR photoresistor. The luminescence was excited by Edison Opto Corporation LEDs with radiation peaks at 375, 400, 460, 550 and 640 nm and a pulsed nitrogen ILGI-503 laser with a wavelength of 331.7 nm.

#### 4. OPTICAL DENSITY STUDY

The optical density spectra of undoped ZnSe nanocrystals are shown in Fig. 2. It has been established that a decrease in the concentration of the initial zinc chloride and sodium selenosulfate from 0.1 g / ml to 0.01 g / ml leads to a shift of the band gap towards high energies from 3.3 to 3.78 eV, which is confirmed by the colloidal solution color change from pale yellow to colorless [11,12,13].

The average radius of the nanoparticles was estimated in the effective mass approximation by the change in the band gap ( $\Delta E_g$ ) compared to bulk crystals, using the formula [9,33]:

$$R = \frac{h}{\sqrt{8\mu\Delta E_g}} \quad (4)$$

Here  $h$  is Planck's constant;  $\mu = ((m_{e^*})^{-1} + (m_{h^*})^{-1})^{-1}$ , where  $m_{e^*} = 0.19m_e$ ,  $m_{h^*} = 0.8m_e$  are, respectively, the effective masses of an electron and a hole in zinc selenide;  $m_e$  is the mass of a free electron;  $\Delta E_g$  is the difference between the band gap in the nanoparticle and the bulk ZnSe crystal (2.68 eV). The results of calculations are presented in Table 1.

SEM images of sample 2 are presented in Fig. 2. The formation of nanoparticles with a size of 10-12 nm observed. The difference between calculated and observed size of crystallites could be explained by agglomeration of smaller grains into larger clusters that are 2-3 times bigger than single nanocrystal. Doping with aluminum or copper shifts the optical absorption edge to lower energies (Fig. 3, Fig. 4). In this case, the magnitude of the shift increases with growth of dopant concentration. A similar low-energy shift is observed in bulk ZnSe: Al and ZnSe: Cu crystals (Fig. 5, Fig. 6).

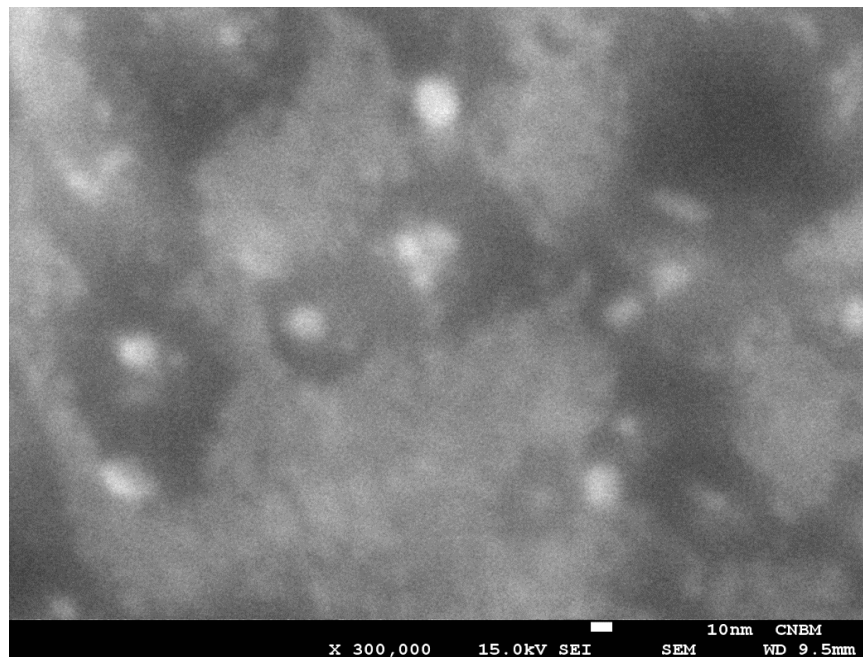


Figure 2. SEM –image of ZnSe nanocrystals (Sample 2)

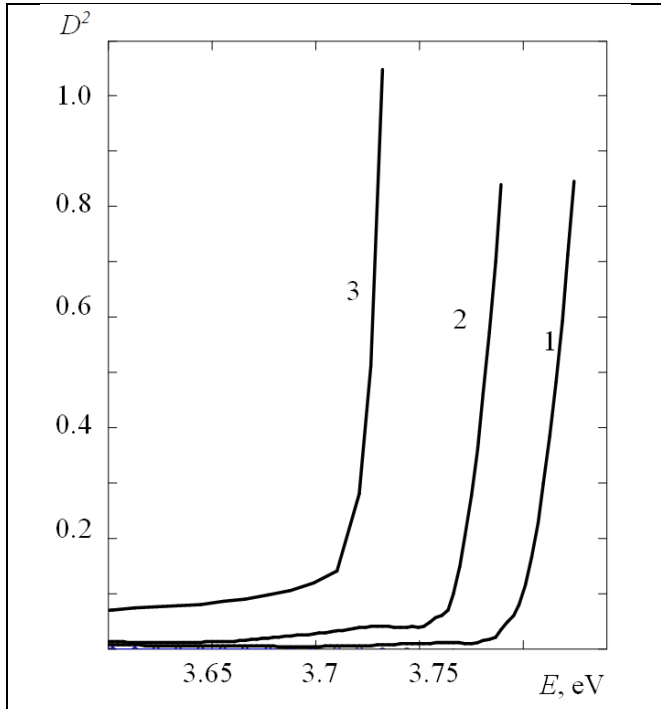


Figure 3. Optical absorption spectra of (1) ZnSe nanocrystals and (2, 3) ZnSe:Al nanocrystals. The Al<sub>2</sub>Cl<sub>3</sub> dopant concentrations are 2% (2) and 5% (3).

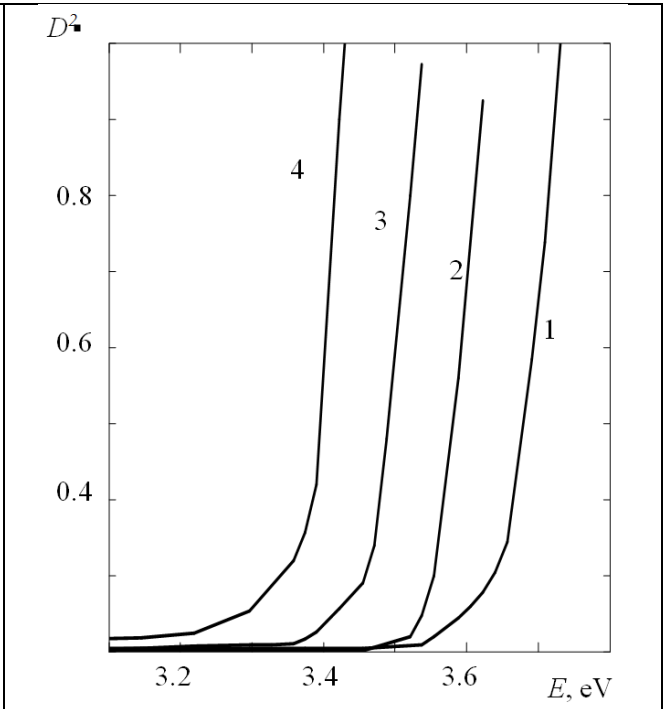


Figure 4. Optical absorption spectra of (1) ZnSe nanocrystals and (2, 3, 4) ZnSe:Cu nanocrystals. The CuCl<sub>2</sub> dopant concentrations are 2% (2), 3% (3) and 5% (4).

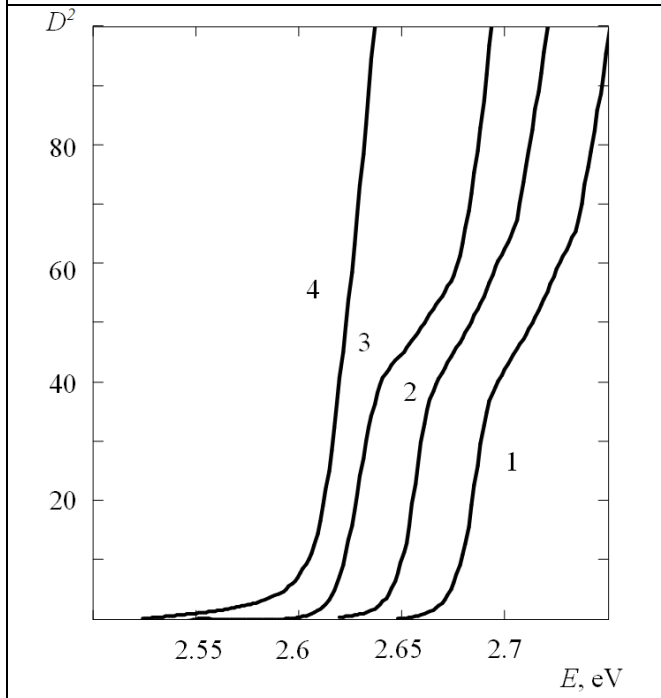


Figure 5. Optical absorption spectra of (1) ZnSe single crystals and (2, 3, 4) ZnSe:Al single crystals. The annealing temperatures are 800 (2), 850 (3) and 900°C (4).

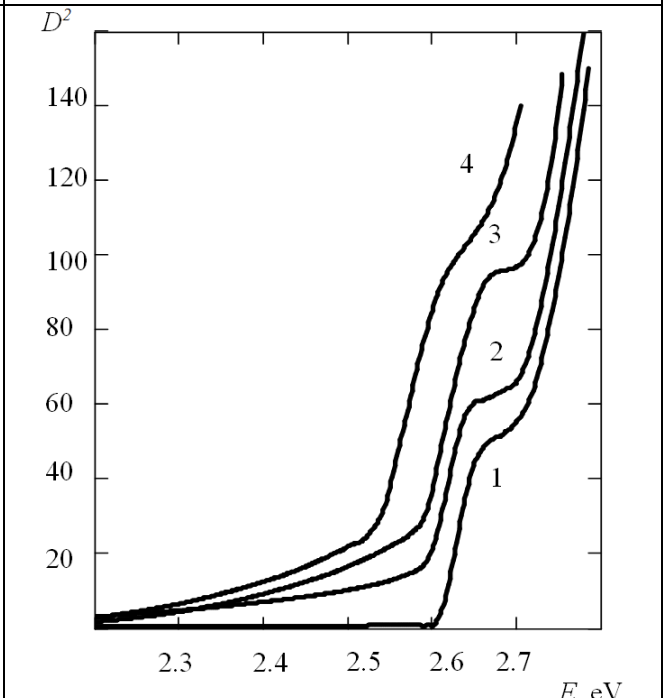


Figure 6. Optical absorption spectra of (1) ZnSe single crystals and (2, 3, 4) ZnSe:Cu single crystals. The annealing temperatures are 800 (2), 850 (3) and 900°C (4).

This shift cannot be explained only by the particle size increase. In bulk crystals, such a shift is explained by inter-impurity Coulomb interaction, which is a characteristic of group III elements [10, 11] and transition element impurities [12–16]. Using the relation [10]

$$\Delta E_g = 2 \cdot 10^5 \left( \frac{3}{\pi} \right)^{1/3} \frac{eN^{1/3}}{4\pi\epsilon_0\epsilon_s}, \quad (5)$$

where:  $e$  – electron charge,  $N$  – concentration of an aluminum or copper impurity in  $\text{cm}^{-3}$ ,  $\epsilon_s = 8.33$  is the static dielectric constant of zinc selenide. The concentration of aluminum and copper in the studied ZnSe: Al nanocrystals (samples 3-4) was calculated from the value of the shift of the band gap between undoped ZnSe nanoparticles (sample 1 or 2). The maximum concentration of optically active aluminum impurity was  $2 \cdot 10^{19} \text{ cm}^{-3}$  in nanocrystals containing 0.002%  $\text{Al}_2\text{Cl}_3$ . When the concentration of  $\text{Al}_2\text{Cl}_3$  decreases to 0.001% the concentration of the optically active aluminum impurity decreases to  $8 \cdot 10^{17} \text{ cm}^{-3}$  respectively. High concentrations of optically active copper impurities indicate the effective incorporation of copper atoms into the zinc sublattice in case of this doping method. The concentration of optically active copper impurity varies from  $2 \cdot 10^{19}$  to  $4 \cdot 10^{20} \text{ cm}^{-3}$  with an increase in the concentration of  $\text{CuCl}_2$  from 0.001 to 0.003% in samples 5-7 [14,15,16].

## 5. INVESTIGATION OF LONG-WAVELENGTH PHOTOLUMINESCENCE

Investigation of ZnSe nanocrystals photoluminescence spectra has shown the presence of broad photoluminescence bands localized in the 550-850 nm region. The change in the temperature of nanocrystals from 300 to 430 K did not cause a shift in the studied spectra. The position of the spectra remained unchanged even with a change in the band gap width of nanocrystals. The presence of a number of bends and a large ( $\sim 150$  nm) half-width of the bands indicate their non-elementary nature. The spectra modeling by elementary Gaussian components program revealed a series of elementary emission lines localized at 580, 600, 630, 680, 700, 750 and 800 nm (Fig. 7a). The identical elementary emission lines were observed earlier in bulk ZnSe single crystals (Fig. 7b) [18,31,32].

Emission at a wavelength of 580 nm appears due to associative native defects ( $V_{\text{Zn}}V_{\text{Se}}$ ). The emission line at a wavelength of 600 nm appears due to associative defects ( $V_{\text{Zn}}D_{\text{Se}}$ ) where the donor is either  $V_{\text{Se}}$  or an uncontrolled donor impurity, an VII group element, for example, Cl, Br, I. The other emission lines were associated with defects ( $V_{\text{Zn}}D_{\text{Zn}}$ ) with different distances between donors and acceptors. Here the donor, according to [18], is the uncontrolled Al, In, Ga impurities [17,18,19].

Doping with aluminium during the growth of nanocrystals leads to an increase of the emission intensity in the 500-1000 nm region. Further increase of the emission intensity with increasing  $\text{Al}_2\text{Cl}_3$  concentration is explained by an increase of the donor impurity concentration in investigated nanocrystals [20,21,22].

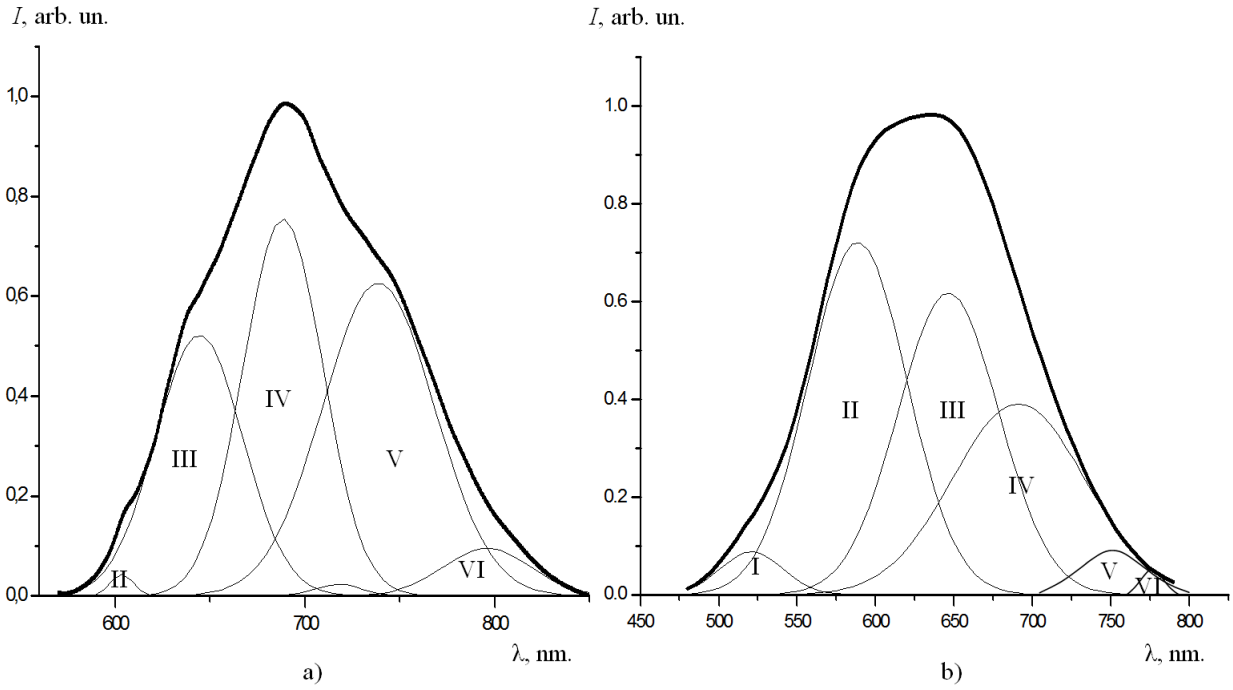


Figure 7. Photoluminescence spectra of (a) ZnSe nanocrystals and (b) single crystals [11]

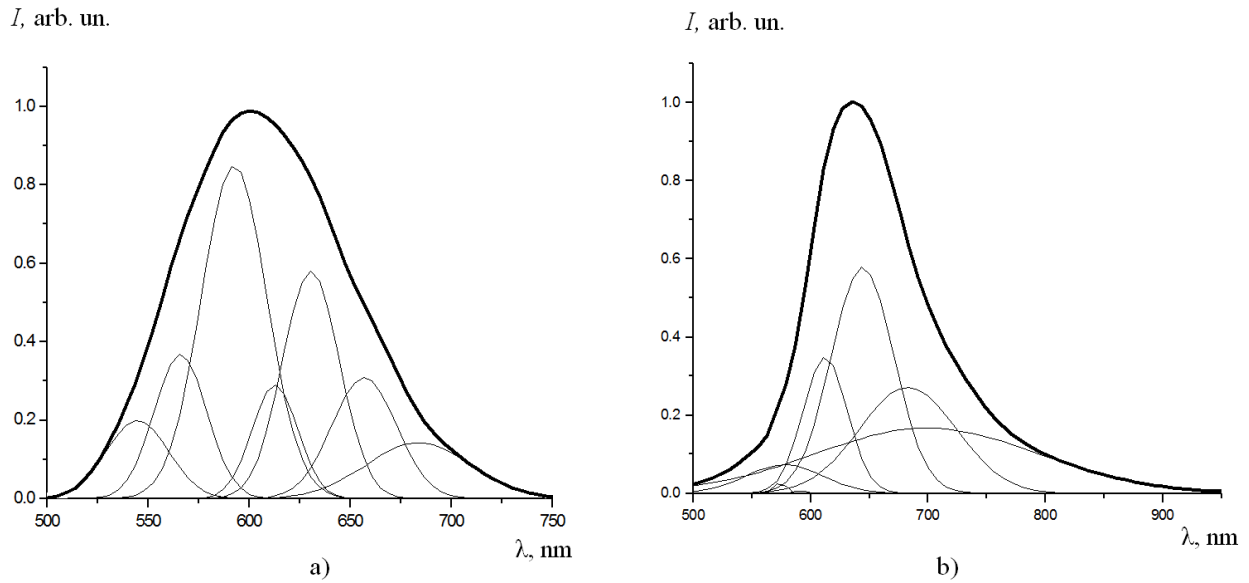


Figure 8. Photoluminescence spectra of (a) ZnSe:Al single crystals and (b) nanocrystals

$I$ , arb. un.

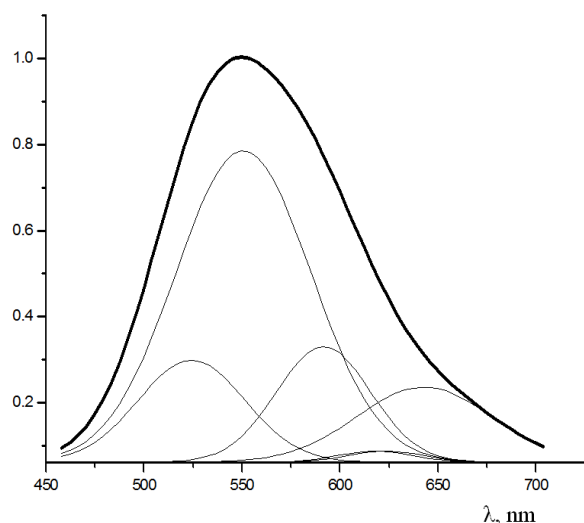


Figure 9. Photoluminescence spectra of ZnSe:Cu nanocrystals (Sample 5)

$I$ , arb. un.

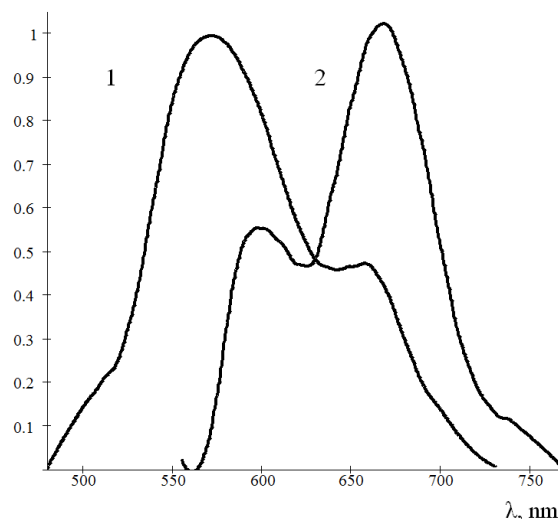


Figure 10. Photoluminescence spectra of ZnSe:Cu single crystals.  $T_{\text{meas}}=77$  (1) and 300 K (2)

In the emission spectra of ZnSe:Al nanocrystals, elementary emission lines are emitted at 580, 600, 630, 680, and 700 nm (Fig. 8 b). The same emission lines were detected in bulk crystals of ZnSe:Al (Fig. 8 a) [28,29,30].

It was found that a change of  $\text{Al}_2\text{Cl}_3$  concentration and the choice of the stabilizing matrix type do not lead to a shift of the elementary and integral emission lines to the short-wave or long-wave region. The change in technological conditions leads to a change in the intensity of the elementary emission lines, which is explained by the redistribution of the concentration of native and impurity defects that create the associative centers. The shift of the emission integrated maximum to the smaller wavelengths region with increasing  $\text{Al}_2\text{Cl}_3$  concentration from 0.001 to 0.002% can be explained by increasing in the intensity of the elementary emission line at 600 nm due to associative defects ( $\text{V}_{\text{Zn}}\text{Cl}_{\text{Se}}$ ) [23,24].

Doping of ZnSe nanocrystals with copper during the growth process leads to a shift of the emission spectra to the shortwave region. The photoluminescence spectra of ZnSe:Cu nanocrystals with a  $\text{CuCl}_2$  concentration of 0.001–0.003% are broad non-elementary emission bands localized in the region of 500–750 nm (Fig. 9). The decomposition of the spectrum into elementary Gaussian components allowed us to identify a series of lines with maxima at 520, 540, 590, 660 nm. Elementary radiation lines with such maxima are not observed in undoped ZnSe nanocrystals. In bulk ZnSe: Cu crystals at  $T = 300$  K, the emission bands at 590 and 660 nm are also detected. In bulk crystals the emission band at 550 nm at  $T = 77$  K is observed. According to [18], the emission lines in bulk crystals and polycrystalline ZnSe films are not connected with isolated  $\text{Cu}_{\text{Zn}}$ , but are caused by the complexes. The emission line at 520 nm is due to transitions ( $\text{Cu}_{\text{Zn}}^-, \text{V}_{\text{Se}}^+$ ). The radiation line at 540–550 nm is associated with transitions within the associative center ( $\text{Cu}_{\text{Zn}}^-, \text{Cl}_{\text{Se}}^+$ ) [19]. The emission line at 660 nm is due to radiative transitions involving doubly charged copper ions within the donor-acceptor pair ( $\text{Cu}_{\text{Zn}}^{2-}, \text{Cl}_{\text{Se}}^+$ ) [19,20]. The emission line at 590 nm is most likely due to transitions involving a doubly charged copper ion and a single-charged selenium vacancy within the center ( $\text{Cu}_{\text{Zn}}^{2-}, \text{V}_{\text{Se}}^+$ ) [18]. A further increase in the concentration of copper chloride to 0.005% and more leads to strong absorption in the near-IR region and concentration quenching of the observed radiation lines, and the colloidal solutions of the nanoparticles become dark gray in color [25,26, 27].

## 6. CONCLUSION

ZnSe, ZnSe: Al, ZnSe: Cu nanoparticles with a diameter of up to 4 nm were successfully synthesized using "green" synthesis method and organic stabilizing agents. The nature of radiation transitions in ZnSe and ZnSe: Al, ZnSe: Cu nanocrystals have been established. It was experimentally confirmed that the emission lines caused by the luminescence on donor – acceptor pairs in nanocrystals are identical to the emission lines in bulk crystals. This proves that ZnSe: Al

and ZnSe: Cu nanocrystals can be effectively used as a material for biomedical visualization, optoelectronics, etc. due to both optical and luminescent properties, and simplicity and low cost of fabrication technology.

### ACKNOWLEDGMENTS

The authors are grateful to Professor I.R. Yatsunsky from Adam Mickiewicz Poznań University for SEM images and discussion of the results.

### REFERENCES

- [1] Gaubas, E., Brytavskiy, I., Ceponis, T., Jasiunas, A., Kalesinskas, V., Kovalevskij, V., Meskauskaitė, D., Pavlov, J., Remeikis, V., Tamulaitis, G., Tekorius, A., „In situ variations of carrier decay and proton induced luminescence characteristics in polycrystalline CdS,” *Journal of Applied Physics* 115, 243507 (2014).
- [2] Gaubas, E., Borschak, V., Brytavskiy, I., Čeponis, T., Dobrovolskas, D., Juršėnas, S., Kusakovskij, J., Smyntyna, V., Tamulaitis, G., Tekorius, A., “Nonradiative and Radiative Recombination in CdS Polycrystalline Structures,” *Advances in Condensed Matter Physics* 2013, 917543 (2013).
- [3] Gaubas, E., Brytavskiy, I., Ceponis, T., Kalendra, V., Tekorius, A., „Spectroscopy of Deep Traps in Cu<sub>2</sub>S-CdS Junction Structures,” *Materials* 5(12), 2597–2608 (2012).
- [4] Peng, X., Schlamp, M. C., Kadavanich, A. V., Alivisatos, A. P., “Epitaxial growth of highly luminescent CdSe/CdS core/shell nanocrystals with photostability and electronic accessibility,” *Journal of the American Chemical Society* 119(30), 7019–7029 (1997).
- [5] Dabbousi, B. O., Rodriguez-Viejo, J., Mikulec, F. V., et al., “(CdSe)ZnS core-shell quantum dots: synthesis and characterization of a size series of highly luminescent nanocrystallites,” *Journal of Physical Chemistry B* 101(46), 9463–9475 (1997).
- [6] Han, D., Song, C., Li, X., “Synthesis and Fluorescence Property of Mn-Doped ZnSe Nanowires,” *J. Nanomaterials* 22, 1-4 (2010).
- [7] Smyntyna, V. A., Skobeeva, V. M., “Photoactivation of luminescence in CdS nanocrystals,” *Beilstein Journal of Nanotechnology* 5, 355-359 (2014).
- [8] Suyver, J. F., van der Beek, T., Wuister, S. F., Kelly, J. J., Meijerink, A., “Luminescence of nanocrystalline ZnSe:Cu,” *Applied Physics Letters* 79, 401 (2001).
- [9] Bouley, J.C., “Blanconnier, P., Hermann, A., “Luminescence in highly conductive n-type ZnSe,” *J. Appl. Phys.* 46(8), 3549- 3555 (1975).
- [10] Vaksman, Yu. F., Nitsuk, Yu. A., Purtov, Yu. N., Shapkin, P. V., “Native and Impurity Defects in ZnSe:In Single Crystals Prepared by Free Growth,” *Semiconductors* 35(8), 920-926 (2001).
- [11] Nitsuk, Yu. A., “Diffusion of chromium and impurity absorption in ZnS crystals,” *Functional Materials* 20(1), 10-14 (2013).
- [12] Nitsuk, Yu. A., Vaksman, Yu. F., “Optical absorption and diffusion of iron in ZnS single crystals,” *Functional Materials* 19(2), 75-79 (2012).
- [13] Nitsuk, Yu. A., „Energy states of a Cr<sup>2+</sup> ion in ZnSe crystals,” *Semiconductors* 47(6), 736-739 (2013).
- [14] Nitsuk, Yu. A., “Optical absorption of vanadium in ZnSe single crystals,” *Semiconductors* 48(2), 142-147 (2014).
- [15] Nitsuk, Yu. A., “Study of the impurity photoconductivity and luminescence in ZnSe:Ni crystals in the visible spectral region,” *Semiconductors* 46(10), 1265-1269 (2012).
- [16] Serdyuk, V. V., Korneva, N. N., Vaksman, Yu. F., “Studies of Long-Wave Luminescence of Zinc Selenide Monocrystals,” *Phys. Stat. Sol.(a)* 91, 173-183 (1985).
- [17] Morozova, N. K., Karetnikov, I. A., Blinov, V. V., Gavrishchuk, E. M., “A study of luminescence centers related to copper and oxygen in ZnSe,” *Semiconductors* 35(1), 24-32 (2001).
- [18] Kukk, P., Palmre, O., Mellikov, E., “The structure of recombination centres in activated ZnSe phosphors,” *Phys. Stat. Sol A* 70(1), 35-42 (1982).
- [19] Bryant, F. G., Manning, P. S., “Radiation damage and decay characteristics of zinc selenide emission bands,” *J. Phys. Chem. Solids.* 35(1), 97-101 (1974).
- [20] Azarov, O. D., Dudnyk, V., Kaduk, O. V., Smolarz, A., Burlibay, A., "Method of correcting of the tracking ADC with weight redundancy conversion characteristic," *Proceedings of SPIE 9816, Optical Fibers and Their Applications 2015*, 98161V (2015).

- [21] Azarov, O. D., Murashchenko, O. G., Chernyak, O. I., Smolarz, A., Kashaganova, G., "Method of glitch reduction in DAC with weight redundancy," *Proceedings of SPIE 9816, Optical Fibers and Their Applications 2015*, 98161T (2015).
- [22] Azarov, O. D., Dudnyk, V., Duk, M., Porubov, D., "Static and dynamic characteristics of the self-calibrating multibit ADC analog components," *Proceedings of SPIE 8698, Optical Fibers and Their Applications 2012*, 86980N (2013).
- [23] Azarov, O. D., Chernyak, A. I., Chernyak, P. A., "Class of numerical systems for pipeline bit sequential development of multiple optoelectronic data streams," *Proceedings of SPIE 4425, Selected Papers from the International Conference on Optoelectronic Information Technologies*, (2001).
- [24] Osadchuk, A., Osadchuk, I., Smolarz, A., Kussambayeva, N., "Pressure transducer of the on the basis of reactive properties of transistor structure with negative resistance," *Proceedings of SPIE 9816, Optical Fibers and Their Applications 2015*, 98161C (2015).
- [25] Osadchuk, O., Osadchuk, V., Osadchuk, I., „The Generator of Superhigh Frequencies on the Basis Silicon Germanium Heterojunction Bipolar Transistors,” *13th International Conference on Modern Problems of Radio Engineering, Telecommunications and Computer Science (TCSET)*, 336-338 (2016).
- [26] Semenov, A. O., Osadchuk, A.V., Osadchuk, I. A., Koval, K. O., Prytula, M. O., "The chaos oscillator with inertial non-linearity based on a transistor structure with negative resistance," *Proceedings of the International Conference Micro/Nanotechnologies and Electron Devices (EDM), 17th International Conference of Young Specialists*, (2016).
- [27] Rovira, R. H., Pavlov, S. V., Kaminski, O. S., Bayas, M. M., "Methods of Processing Video Polarimetry Information Based on Least-Squares and Fourier Analysis," *Middle-East Journal of Scientific Research* 16 (9), 1201-1204 (2013).
- [28] Zabolotna, N. I., Pavlov, S. V., Ushenko, A. G., Karachevtsev, A. O., Savich, V. O., et al. "System of the phase tomography of optically anisotropic polycrystalline films of biological fluids," *Proceedings of SPIE 9166, Biosensing and Nanomedicine VII*, 916616 (2014).
- [29] Zabolotna, N. I., Pavlov, S. V., Ushenko, A. G., Sobko, O. V., Savich, V. O., „Multivariate system of polarization tomography of biological crystals birefringence networks," *Proceedings of SPIE 9166, Biosensing and Nanomedicine VII*, 916615 (2014).
- [30] Wójcik, W., Smolarz, A., [Information Technology in Medical Diagnostics], London, July 11, Taylor & Francis Group CRC Press Reference (2017).
- [31] Vassilenko, V., Valtchev, S., Teixeira, J. P., Pavlov, S., "Energy harvesting: an interesting topic for education programs in engineering specialities," *Internet, Education, Science (IES-2016)*, 149-156 (2016).
- [32] Krak, Y. V., Barmak, A. V., Bagriy, R. A., Stelya, I. O., "Text entry system for alternative speech communications," *Journal of Automation and Information Sciences* 49(1), 65–75 (2017).
- [33] Kryvonos, Iu. G., Krak, Y. V., Barmak, O. V., Bagriy, R. O., "Predictive text typing system for the Ukrainian language," *Cybernetics and systems analysis* 53(4), 495-502 (2017).